Spatial selection of mixed states of quantum systems

B. D. Agan'ev, M. B. Gornyĭ, and B. G. Matisov

Leningrad Polytechnical Institute
(Submitted 13 July 1988)
Zh. Eksp. Teor. Fiz. **95**, 81–92 (January 1989)

The selection kinetics of mixed states of quantum systems is investigated. Various selection modes are considered. Expressions have been found for the transverse magnetization and its flux density in the system. The effect of elastic collisions on these quantities is discussed. The phenomenon of population trapping in a three-level system is considered. It is shown that this causes a maximum transverse magnetization flux in the system. The effect of boundary conditions on selection efficiency is considered. The nature of spatial oscillations of transverse magnetization and the efficiency of various selection modes are discussed.

1. INTRODUCTION

In recent years, researchers have been paying much attention to optically stimulated drift (OSD) of gas[1,2] in a coherent electromagnetic radiation field. OSD is caused by velocity-selective interaction of gas atoms (molecules) with the coherent field.

An effect related to OSD is the spatial selection of quantum states (SQS) of atoms and molecules in a coherent electromagnetic field.[3,4] In both cases the effect is manifested by a macroscopic flow of atoms. However, while OSD separates binary gas mixtures into their components through the different scattering cross sections of active atoms in the ground and excited states, SQS is associated with spatial separation of active atoms by different quantum states[3] or with the separation of an initially noncoherent mixture of quantum states into two coherent components that are opposite in phase.[4] Consequently, we can talk about the selection of pure states and the selection of mixed states. This paper describes the kinetics of the latter selection mode.

The causes of spatial selection of pure states are known[3]: when a coherent electromagnetic field in the form of a traveling monochromatic wave is applied to a transition between levels m and n, the Maxwell velocity distributions of particles at these levels are deformed. The velocity-selective interaction of the atoms with the coherent electromagnetic field gives rise to an asymmetric Bennett structure of these distributions, which leads to transport of atoms with states $|m>$ and $|n>$ in opposite directions. The atoms are spatially separated by states in a bounded volume. The main condition making SQS possible is a sufficient lifetime ($\tau \gtrsim 10^{-4}$ s) in each of the separated states, to ensure that the magnitude of spatial separation $l > \tau v_T$ is comparable to the characteristic dimension L of the volume occupied by the gas.

The off-diagonal element f^{mn} of the density matrix (coherence) of the active atoms is a dispersive function of velocity,[4] in contrast to the populations of the states $|m\rangle$ and $|n\rangle$, whose velocity dependence has the form of a Maxwell curve with Bennett holes. Therefore, while the transport of populations and spatial selection of pure states are possible only off resonance, the transfer of coherence and selection of mixed states can occur and are maximal precisely at resonance—in the absence of particle flows in each state. A clear interpretation of this phenomenon can be easily provided in the case of transitions between Zeeman-structure levels.[4] In a frame of reference rotating synchronously with the magnetic-field vector of an electromagnetic wave, there is a predominant orientation of transverse atomic spin moments along the magnetic-field-intensity vector of the wave, i.e., coherence is established in the spin system. The number of atoms traveling in the direction of the wave vector of the electromagnetic radiation is then equal at resonance to the number of atoms traveling in the opposite direction. However, the atoms moving along the electromagnetic field interact coherently with the field for a longer time and, consequently, transfer a larger transverse angular momentum or coherence. In a limited volume, the macroscopic transfer of coherence leads to spatial separation of the mixture of quantum states $|m\rangle$ and $|n\rangle$ into coherent components and can be observed by known methods.[5]

2. RADIO-STIMULATED TRANSPORT OF MIXED STATES

Radio-stimulated transport (RST) of coherence is the first representative of a broad class of phenomena caused by the transfer of coherence from the electromagnetic field to an atomic (molecular) system and leading to spatial selection of mixed states.

To describe the phenomenon, we consider low-density vapor of active material whose spectral transitions lie in the radio-frequency region of the spectum ($\omega_{21} \sim 10^6$–10^{13} s^{-1}). These transitions correspond to Zeeman levels sufficiently broadened by a constant magnetic field, to hyperfine and fine structure levels, and to transitions between rotational levels of molecules in the millimeter and centimeter bands. We assume a difference in the populations of states $|1\rangle$ and $|2\rangle$, which is due to the Boltzmann factor $\exp(-\hbar\omega_{21}/T)$ (as in the case of thallium vapor), or is produced by noncoherent optical pumping (as in the case of alkaline vapors). Quantum kinetic equations describing the density-matrix dynamics of active atoms are given for the latter case in Ref. 3. Their stationary spatially homogeneous solution in a collisionless situation leads to the following expressions for the tranverse-magnetization flux density components:

$$j_{zx}(\Omega) = n\mu_B \frac{wU}{w+\gamma}(w+\Gamma)J_1,$$
$$j_{zy}(\Omega) = n\mu_B \frac{wU}{w+\gamma}(\Omega J_1 - kJ_2). \qquad (2.1)$$

Here w is the pumping rate, $\gamma = T_1^{-1}$ and $\Gamma = T_2^{-1}$ are axial and transverse relaxation rates, $U = 2|U_{21}|/\hbar$ is the Rabi frequency determined by the matrix element U_{21} of the magnetic dipole interaction, Ω and k are the radiofrequency

 0038-5646/89/010046-07$04.00

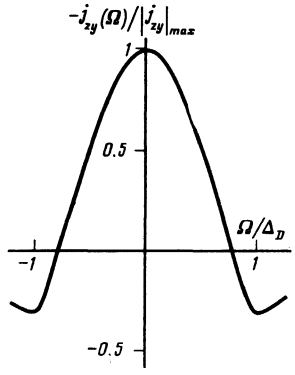

FIG. 1. Transverse magnetization flux in RST as a function of radiofrequency detuning: $U = w = 10^2\gamma$, $kv_T = 10^3\gamma$.

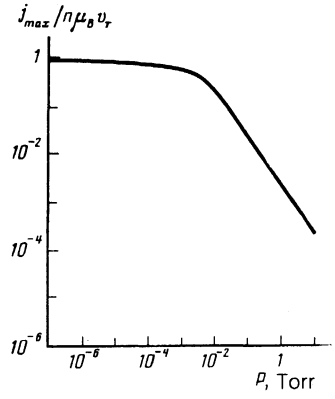

FIG. 3. The amplitude of transverse magnetization flux as a function of buffer-gas pressure: $U = w = 10^2\gamma_0$.

detuning and the wave vector, μ_B is the Bohr magneton,

$$J_n = J_n(\Gamma_0, \Omega) = \int_{-\infty}^{+\infty} \frac{v_z^n \mathcal{M}(v_z)\, dv_z}{\Gamma_0^2 + \Delta^2},$$
$$\Gamma_0^2 = (\Gamma + w)^2 + \frac{\Gamma + w}{\gamma + w} U^2, \quad \Delta = \Omega - kv_z, \tag{2.2}$$

and $\mathcal{M}(\mathbf{v})$ is a Maxwell distribution. We assume that the z axis is parallel to the wave vector and the y axis points along the rotating magnetic field intensity vector of the radio wave. We employ here the usual expressions for the specific magnetization m_i and for the magnetization flux density j_{ik} in terms of density-matrix components f^{mn} (Ref. 6):

$$m_- = {}^1/_2(m_x - im_y) = -n\mu_B f^{12},$$
$$m_z = n\mu_B f, \quad f = f^{22} - f^{11}, \tag{2.3}$$
$$j_{ik} = \int v_i m_k(\mathbf{v})\, d^3v, \quad i, k = x, y, z.$$

As discussed in the Introduction, j_{zy} is the only nonzero flux component at resonance ($\Omega = 0$). Figure 1 shows the transverse magnetization flux as a function of radiofrequency detuning. It is convenient to characterize the magnitude of transverse magnetization flux by the value of velocity $V = j_{zy}/n\mu_B$. For parameter values that are typical of optical pumping experiments, $\gamma \sim \Gamma \sim 10$–$10^2$ s^{-1} and $w \sim U \sim 10^4$ s^{-1}, flux velocity is of the order of thermal velocity: $V \sim 0.4 v_T$. Thus, coherence transfer occurs over a macroscopic distance of the order of

$$l \sim V/\Gamma \sim 10^2 - 10^3 \text{ cm}.$$

Taking collisions of the active atoms with the buffer-gas atoms into account[7] yields for the components of the transverse-magnetization flux-density tensor expressions that are considerably more complex than (2.1):

$$j_{zx}(\Omega) = (w+\Gamma+\nu)\,[\nu J_1' M_x(\Omega) + \alpha(\nu M_z(\Omega) + wM_0)] + \nu(kJ_2' - \Omega J_1')\, M_y(\Omega),$$
$$j_{zy}(\Omega) = \nu(w+\Gamma+\nu+\alpha U) J_1' M_y(\Omega) + (\Omega J_1' - kJ_2')\,[\nu M_x(\Omega) + \alpha(\nu M_z(\Omega) + wM_0)], \tag{2.4}$$

where

$$J_n' = J_n(\Gamma_\nu, \Omega), \quad \Gamma_\nu^2 = (w+\Gamma+\nu)(w+\Gamma+\nu+\alpha U),$$
$$M_i(\Omega) = \int m_i(\mathbf{v}, \Omega)\, d^3v \tag{2.5}$$

is the vapor magnetization, $M_0 = n\mu_B$, $\alpha = U/(w + \gamma + \nu)$, and ν is the gaskinetic frequency of elastic collisions of active atoms with buffer atoms (in the strong collisions model).

The magnetization flux as a function of pressure (collision frequency ν) is illustrated in Figs. 2 and 3.

In the limit of high collision frequencies, the expressions for the fluxes become simpler and assume the form

$$j_{z-} = \frac{1}{2}(j_{zx} - ij_{zy}) \approx n\mu_B v_T \frac{wU}{4\nu(w+\gamma)} \frac{kv_T[\Omega + i(w+\Gamma)]}{\Gamma_0^2 + \Omega^2}. \tag{2.6}$$

Thus, the transverse-magnetization flux is inversely proportional to pressure. Nevertheless, the graph in Fig. 3 shows that radio-stimulated coherence transfer still remains significant at collision frequencies $\nu \sim 10^7$–10^8 s^{-1}, which correspond to pressures of the order of several torr.

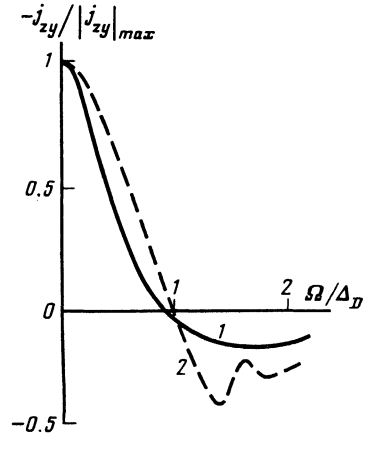

FIG. 2. The effect of buffer gas pressure on the transverse magnetization flux in RST: $U = w = 10^2\gamma_0$; 1—$P = 10^{-3}$ Torr, 2—$P = 10^{-2}$ Torr.

3. TRANSPORT OF MIXED STATES IN TWO-BEAM EXCITATION

In this section we consider a more complex method of exciting coherence flows. However, as further discussion will show, the method will lead to a more complete spatial selection of mixed states.

To be specific, we consider low-density vapor of an ac-

tive element, assuming that subject to separation are long-lived states $|1\rangle$ and $|2\rangle$, while the excited state $|3\rangle$ is short-lived. Coherent electromagnetic fields in the form of plane monochromatic waves with Rabi frequencies U_1 and U_2 and detunings $\Omega_1 = \omega_1 - \omega_{31}$ and $\Omega_2 = \omega_2 - \omega_{32}$ are applied to the adjacent transitions 1–3 and 2–3 respectively.

Velocity selection of the interactions with coherent fields leads to a Bennett deformation of the Maxwell distributions of the particles at levels 1 and 2 and to the spatial transport of pure quantum states.[3] As indicated in Ref. 3, spatial selection of pure states is most effective when the wave vectors and field detuning meet the following conditions:

$$\begin{aligned} &k_1 \text{ is collinear with } \mathbf{k}_2, \\ &\Omega_1 = -\Omega_2 \operatorname{sign}(\mathbf{k}_1, \mathbf{k}_2). \end{aligned} \tag{3.1}$$

Another aspect of the described phenomenon consists in the transfer of coherence of the electromagnetic fields to the atomic system and in the appearance of a macroscopic flow of low-frequency coherence f^{12}. The transitions 1–3 and 2–3 and the transition 1–2 may lie in different regions of the spectrum, for example in the optical and radiofrequency bands, respectively. In that case, the coherent optical fields U_1 and U_2 will excite a macroscopic flow of radiofrequency coherence. To be specific, we will consider just these frequency ranges in the following discussion, although the qualitative aspect of the phenomenon does not depend on such a choice. A system of quantum kinetic equations for the density matrix of active atoms, corresponding to the case under consideration, is given in Ref. 3.

As we have found in considering RST, the collisions of active atoms with buffer atoms decrease the efficiency of SQS by reducing the degree to which the density matrix of the active gas deviates from equilibrium. Therefore we shall consider from now on only the most interesting situation, in which we can neglect relaxation via collsions of the above type.

Let, as before, $\Delta_i = \Omega_i - \mathbf{k}_i \cdot \mathbf{v}$; the quantities

$$W_i = U_i^2 A/(A^2 + 4\Delta_i^2), \quad i = 1, 2$$

have the meaning of coherent-excitation rates that depend on the detuning Ω_i of the employed radiations and on the velocities $\mathbf{v}$ of the active atoms. Even though the general spatially homogeneous stationary solution can be written for any Rabi frequency, we present expressions for specific magnetizations only for the case of not too high Rabi frequencies. This option has been dictated by both the complexity of the expression for $\mathbf{m}(\mathbf{v})$ in general, and by the not unimportant consideration that, according to analysis, the optimal (for the production of largest macroscopic magnetization fluxes) Rabi frequencies lie in the region where the characteristic rates W_i of coherent excitation are small in comparison to rate A of spontaneous relaxation from the excited state $|3\rangle$.

For the above limitations, we find (for the case $U_1 = U_2 \equiv U$)

$$\begin{aligned} m_x &= \frac{\bar{\Delta}(Qm_z + \tilde{Q}m_0) + wEm_0}{E^2 + \bar{\Delta}^2}, \\ m_y &= \frac{\bar{\Delta}(wm_0 - \tilde{w}m_z) - QEm_z}{E^2 + \bar{\Delta}^2}, \\ m_z &= m_0 \left[\frac{\tilde{w}}{\varepsilon} \left(1 - \frac{E}{\varepsilon} \frac{w\varepsilon + Q^2}{E^2 + \bar{\Delta}^2} \right) + \frac{\bar{\Delta}}{\varepsilon A} \frac{W_1^2\Delta_1 + W_2^2\Delta_2}{E^2 + \bar{\Delta}^2} \right] \end{aligned} \tag{3.2}$$

where $m_0 = n\mu_B \mathscr{M}(v_z)$, $\varepsilon = w + \gamma$, $E = w + \Gamma$, and $\tilde{E} = (E^2 + Q^2 E/\varepsilon)^{1/2}$. Here we designate $\bar{\Delta} = \Delta_1 - \Delta_2$, $w = (W_1 + W_2)/2$, $\tilde{w} = (W_1 - W_2)/2$, $Q = (W_1\Delta_1 + W_2\Delta_2)/A$, and $\tilde{Q} = (W_1\Delta_1 - W_2\Delta_2)/A$.

In contrast to the RST case discussed above, the low-frequency coherence f^{12} and the corresponding transverse magnetization $m_- = -n\mu_B f^{12}$ appear here because the atomic system is acted upon not by a single coherent field on the low-frequency transition 1–2, but by two fields applied to adjacent optical transitions 1–3 and 2–3. The frequencies of these fields are much higher than that of the 1–2 transition, so that the excitation of transverse magnetization can be interpreted as a transfer, to the atomic system, of the coherence of a combined electromagnetic field at the frequency $\omega_1 - \omega_2$.

Analysis shows that the described two-frequency excitation of transverse magnetization is most efficient with parallel pumping beams ($\mathbf{k}_1 \| \mathbf{k}_2$) that satisfy the synchronism condition:

$$\Omega_1 = |\Omega_2| \equiv \Omega. \tag{3.3}$$

In this case, there exists a region of optimal pumping rates that increase the transverse and axial magnetizations to values comparable to m_0, and provide transverse-magnetization fluxes of considerable magnitude. The optimality conditions depend on the relation between the detunings. When one wing of the Maxwell rate distribution the populations of states $|1\rangle$ and $|2\rangle$ is excited ($\Omega_1 = \Omega_2$), the optimal Rabi frequencies of the optical field are of the order of $U \sim (q/k)^{1/2} A$ ($k_2 \approx k_1 \equiv k$, $q = k_1 - k_2 \ll k$). However, when the fields simultaneously deform both wings of the distribution ($\Omega_1 = -\Omega_2 \equiv \Omega$), the optimal Rabi frequencies are $U \sim (\Omega^2 + q^2 A^2/k^2)^{1/2}$.

We must emphasize that in the case of oppositely directed beams there are no optimal frequencies and the specific magnetizations are always small in comparison to the quasi-equilibrium magnetization. Therefore, from now on, we consider only parallel beams.

Satisfaction of the synchronism (3.3) and optimality conditions considerably simplifies the general expressions (3.2) for the specific magnetization. If the detuning does not

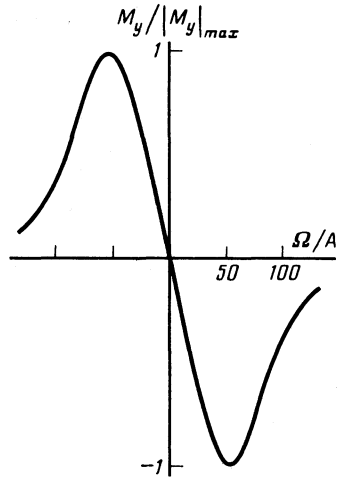

FIG. 4. Frequency dependence of transverse magnetization under two-beam excitation: $U = A/4.5 = 2 \cdot 10^2 q v_T$, $\gamma = 3 \times 10^{-3} q v_T$.

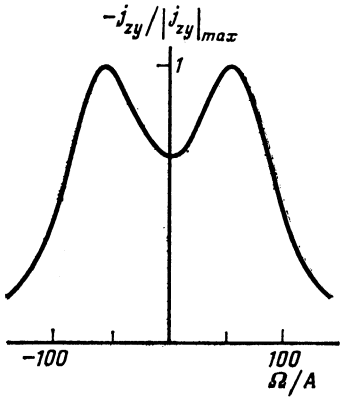

FIG. 5. Frequency dependence of transverse magnetization flux under two-beam excitation: $U = A/4.5 = 2\cdot 10^2\, qv_T$, $\gamma = 3\cdot 10^{-3}\, qv_T$.

exceed the width of the excited state, we can write these expressions in the form

$$m_x = \frac{w(\varepsilon E + 4w^2\Delta^2/A^2)}{\varepsilon(E^2+\tilde{\Delta}^2)+4w^2\Delta^2/A^2}\, m_0,$$

$$m_y = \frac{\varepsilon w\tilde{\Delta}}{\varepsilon(E^2+\tilde{\Delta}^2)+4w^2\Delta^2/A^2}\, m_0, \qquad (3.4)$$

$$m_z = 2\frac{\Delta}{A}\,\frac{w^2\tilde{\Delta}}{\varepsilon(E^2+\tilde{\Delta}^2)+4w^2\Delta^2/A^2}\, m_0.$$

Here $\tilde{\Delta} = -qv_z$ for pumping in one wing and $\tilde{\Delta} = 2\Omega - qv_z$ for pumping in different wings; $\Delta = (\Omega_1+\Omega_2)/2 - kv_z$.

The integrated magnetization (the magnetic moment per unit volume of gas) is computed from formula (2.5). The results of the computation are shown in Fig. 4. Note that transverse magnetization is a maximum when the conditions for two-photon and two-step[8] resonances are simultaneously met (i.e. in the case of parallel beams with $\Omega_1 = \Omega_2 = 0$). Here we have coherent trapping of the populations,[9] i.e., the capture of active atoms into a coherent superposition, not connected to the optical level 3, of lower states $|1\rangle$ and $|2\rangle$. Coherent population trapping strongly suppresses the atomic system's ability to emit or absorb photons. This is achieved at the price of inducing a maximum possible transverse magnetization in the system.

The distribution of the specific magnetization in velocity is asymmetric by virtue of the selective nature of interaction of atoms with coherent radiation, as discussed in the Introduction. The asymmetry gives rise to a macroscopic magnetization flux along the pumping beam. In this process, one of the flux-density components (j_{zy}) is different from zero even at resonance. Figure 5 shows its dependence on the detuning for $\Omega_1 = \Omega_2 \equiv \Omega$, computed from Eqs. (2.3) and (3.2). This dependence is qualitatively in agreement with the results of the corresponding computations made for the case of radio-stimulated transport.

4. MAGNETIZATION WAVES IN GASES

The wave nature of low-lying energy states in ordered spin systems has been known for a long time and is well understood. Less obvious is the fact that spin-wave states can be observed in disordered systems and even in a gas at temperatures far from degeneracy. We will demonstrate this fact in the concrete case of a radio-optical resonance in rarefied vapor of an alkaline element.

As shown in Ref. 7, kinetic quantum equations for the density matrix of active atoms can be written in this case in the form of equations for the specific magnetization $\mathbf{m}(t,\mathbf{r},\mathbf{v})$ in a rotating coordinate frame

$$\frac{\partial \mathbf{m}}{\partial t} + (\mathbf{v}\nabla)\mathbf{m} + \Gamma\mathbf{m} = [\mathbf{O}\mathbf{m}] + \hat{S}\mathbf{m} + w\mathbf{M}_0\mathcal{M}(\mathbf{v}), \qquad (4.1)$$

where Γ is the diagonal relaxation tensor, $\hat{S}$ is the collision operator, $\mathbf{O} = U\mathbf{e}_y + \Delta\mathbf{e}_z$ is the generalized Rabi frequency, $\mathbf{M}_0 = n\mu_B\mathbf{e}_z$, and $\mathbf{e}_z = \mathbf{k}/k$.

In the presence of relaxation, spin-wave states are subject to damping and are well defiend only for the case of small decrements. Therefore, limiting the example to the collisionless case and assuming that all relaxation processes can be neglected, we write the equations for the spin-wave perturbation $\delta\mathbf{m}$ in the form

$$\left(\frac{\partial}{\partial t} + \mathbf{v}\nabla\right)\delta\mathbf{m} = [\mathbf{O}\delta\mathbf{m}]. \qquad (4.2)$$

The solutions in the form of plane waves $\delta\mathbf{m} \propto e^{i(\mathbf{qr}-\omega t)}$ correspond to dispersion laws

$$\omega_1 = \mathbf{qv}, \qquad \omega_\pm = \mathbf{qv} \pm \sigma \quad (\sigma^2 = U^2+\Delta^2), \qquad (4.3)$$

which determine the possible oscillation modes.

Of interest is the evolution of the initial perturbation. In the general case, propagation of perturbations of any polarization excites typically not one but all three oscillation modes. Only spin waves with a definite polarization are elementary waves, i.e, waves obeying a definite dispersion law.

An arbitrary initial perturbation of magnetization evolves in time in the form of the following superposition of elementary spin waves:

$$\delta\mathbf{m}(t,\ \mathbf{r},\ \mathbf{v}) = e^{iq(\mathbf{r}-\mathbf{v}t)}[M_1\mathbf{e}_u + e^{-i\sigma t}M_+(\mathbf{e}_\Delta - i\mathbf{e}_x) + e^{i\sigma t}M_-(\mathbf{e}_\Delta + i\mathbf{e}_x)], \qquad (4.4)$$

where we have introduced two mutually orthogonal unit vectors $\mathbf{e}_u = \sigma^{-1}\mathbf{O}$ and $\mathbf{e}_\Delta = [\mathbf{e}_u \times \mathbf{e}_x]$. The coefficients M_1 and $M_\pm$ are determined by the initial conditions. Equations (4.4) show that the oscillations ω_1 are polarized along the vector $\mathbf{e}_u$, while the two modes ω_+ and ω_- have polarizations along $\mathbf{e}_- = \mathbf{e}_\Delta - i\mathbf{e}_x$ and $\mathbf{e}_+ = \mathbf{e}_\Delta + i\mathbf{e}_x$ respectively. Thus, there is a rigid bond between the polarization of spin waves and the dispersion law.

In addition, it follows from Eq. (4.4) that a particular polarization possessed by an initial perturbation is preserved throughout the process, and that the perturbation evolves as an elementary spin wave without exciting other modes of magnetization oscillations. At the same time, the initial magnetization perturbation, which is a mixture of oscillations with various polarizations, continues to be a mixture of the same polarizations.

As in the case of electromagnetic waves, magnetization waves are subject to interference and diffraction. However, their analysis is made significantly more complex by the fact that magnetization waves have three elementary polarizations (and not two, as do electromagnetic waves). We shall

consider some consequences of this interference in the next section.

5. SPATIAL SELECTION OF MIXED STATES

In this section we present the quantitative description of SQS methods discussed above. We shall first turn to the RST phenomenon. Consider a gas cell filled with the vapor of an active element whose atoms interact with coherent electromagnetic radiation of frequency $\omega = \Omega + \omega_{21}$. The initial population inversion of the 1–2 transition is ensured by the Boltzmann factor or by noncoherent optical pumping. In the latter case, the determination of the spatial distribution of transverse magnetization (of the radiofrequency coherence) reduces to the solution of quantum kinetic equations[3] under appropriate boundary conditions on the cell walls.

We consider a cell of length $2L$. We assume that a traveling electromagnetic wave propagates parallel to the z axis, so that the specific-magnetization components m_z and m_- vary only along z. We choose "specularly-noncoherent" reflection boundary conditions:

$$\begin{aligned} m_z(v_z, \pm L) &= m_z(-v_z, \pm L), \\ m_-(v_z, -L) &= m_-(-v_z, L) = 0, \end{aligned} \tag{5.1}$$

corresponding, at the tube wall, to a fully relaxed transverse moment and a conserved axial moment of the active atom. As a result, for the components of the integrated transverse magnetization

$$M_-(z) = {}^1/_2(M_x - iM_y) = \int m_-(\mathbf{v}, z)\, d^3v \tag{5.2}$$

we obtain in the stationary case

$$\begin{aligned} M_x(z) = n\mu_B \frac{w}{w+\gamma} \int_0^\infty dv_z \mathcal{M}(v_z) \Big[& \frac{\varepsilon U}{\varepsilon^2 + \delta_+^2} + \frac{\varepsilon U}{\varepsilon^2 + \delta_-^2} \\ & + e^{-\varepsilon z/v_z} \left(f_2^+ \sin \frac{z\delta_+}{v_z} - f_3^+ \cos \frac{z\delta_+}{v_z} \right) \\ & - e^{\varepsilon z/v_z} \left(f_2^- \sin \frac{z\delta_-}{v_z} + f_3^- \cos \frac{z\delta_-}{v_z} \right) \Big], \end{aligned} \tag{5.3}$$

$$\begin{aligned} M_y(z) = n\mu_B \frac{w}{w+\gamma} \int_0^\infty dv_z \mathcal{M}(v_z) \Big[& \frac{U\Delta_+}{\varepsilon^2 + \delta_+^2} + \frac{U\Delta_-}{\varepsilon^2 + \delta_-^2} \\ & + e^{-\varepsilon z/v_z} \left\{ \frac{U}{\Delta_+} f_1^+ - \frac{\Delta_+}{U} \left(f_2^+ \cos \frac{z\delta_+}{v_z} + f_3^+ \sin \frac{z\delta_+}{v_z} \right) \right\} \\ & + e^{\varepsilon z/v_z} \left\{ \frac{U}{\Delta_-} f_1^- - \frac{\Delta_-}{U} \left(f_2^- \cos \frac{z\delta_-}{v_z} - f_3^- \sin \frac{z\delta_-}{v_z} \right) \right\} \Big]. \end{aligned}$$

The notation, as well as the expressions for the coefficients $f_i^\pm$, are the same here as in Ref. (3).

It is natural to expect that in the case of boundary conditions of "specularly-coherent" reflection from the cell walls

$$m_i(v_z, \pm L) = m_i(-v_z, \pm L), \quad i = x, y, z, \tag{5.4}$$

which correspond to conservation of both the axial and transverse moments of the active atoms colliding with a wall provided with a protective coating, one can obtain a large transverse-magnetization amplitude. Calculations confirm this expectation. The resulting expressions for the transverse-magnetization components have the form (5.3) given above, albeit with somewhat different expressions for the coefficients $f_i^\pm$ (Ref. 7).

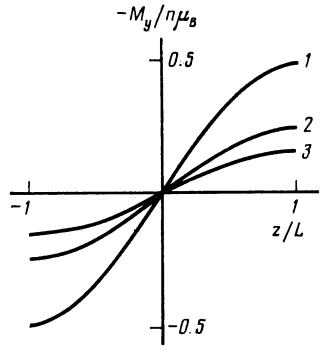

FIG. 6. Selection of mixed states in RST: $2L = \lambda/2$; 1—$U = 4w = 20\gamma$, 2—$U = w = 5\gamma$, 3—$U = w = \gamma$.

Since the distinctive features of the spatial distribution of the transverse magnetization, described below, are most pronounced in the case of "specularly-coherent" reflection of the atoms from the walls, we cite the results of numerical computation using Eq. (5.3) for this case. Figures 6–8 show the transverse magnetization as a function of z for the case of resonance ($\Omega = 0$) of the electromagnetic field at the transition $|1\rangle$–$|2\rangle$. In this case, components j_{zx} and j_{zz} of the macroscopic magnetization flux are absent, so that the axial magnetization M_z and the transverse magnetization M_x are constant over the length of the cell. At the same time, the component j_{zy} reaches a maximum at resonance, which is the main reason why M_y depends strongly on the spatial coordinate.

First of all, the function $M_y(z)$ is odd. This function is typically monotonic so long as not more than one half-wave fits within the length of the cell. We can speak here of separation of mixed states into two components opposed in phase. In such a case, the left and right halves of the cell turn out to be oppositely magnetized in the transverse direction. The maximum possible magnetization increase as both L/λ and w/U increase.

As soon as more than two half-waves can fit within the length of the cell, the spatial dependence of the transverse magnetization becomes much more complex. The gas vol-

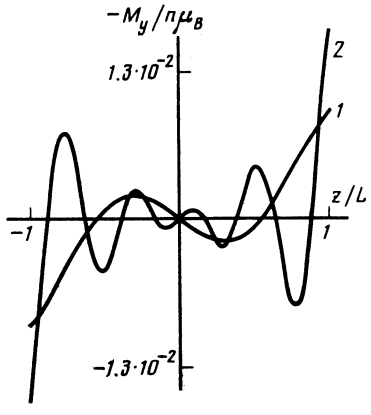

FIG. 7. Spatial oscillations of transverse magnetization in RST: $w = \gamma$, $U = 4w$; 1—$2L = \lambda$, 2—$2L = 4\lambda$.

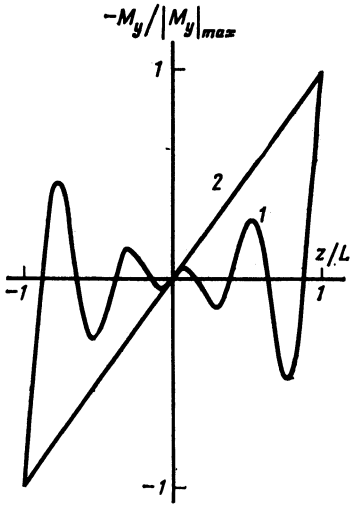

FIG. 8. Magnetization oscillation damping in the field of a strong electromagnetic wave: $2L = 4\lambda$, $w = \gamma$; 1—$U = 4\omega$, 2—$U = 8\cdot 10^3 w$.

ume breaks up into alternating oppositely magnetized layers. The thickness of each layer and its average magnetization increase with distance from the center of the cell. This pattern of transverse magnetization oscillations is determined by the presence of a reverse magnetization flux from the cell walls. We can point to two mechanisms responsible for the onset of radiofrequency-coherence (or transverse-magnetization) oscillations. The first is that the radiofrequency electromagnetic field imposes phases upon the transverse moments of individual atoms. If this mechanism were the sole determinant of the phase of the transverse magnetization, the nodes and antinodes of M_y would correspond precisely to the nodes and antinodes of the radiofrequency field and would be equidistant. However, the reverse magnetization flux from the tube walls causes interference between the forward and reverse spin waves. This interference represents an additional mechanism determining the coherence phase; it makes the locations of the nodes of M_y dependent on the dimensions of the cell. We must also take it into account that the spin waves under consideration are damped. This is manifested by the uneven distribution of the transverse-magnetization nodes along the cell axis.

With increasing Rabi frequency, the frequency of the oscillations increases but their amplitude decreases. Therefore, the breakdown into alternating layers vanishes at Rabi frequencies that exceed the Doppler width of the 1–2 transitions (Fig. 8). Instead, a monotonic magnetization distribution is set up in the cell, corresponding to the separation of the initially noncoherent mixture of quantum states into two coherent components which are, on the average, in counterphase.

We turn now to the spatial distribution of mixed states in the case of two-beam excitation. The solution of the quantum kinetic equations[3] describing the reaction of an atomic system to interaction with coherent optical fields at the adjacent transitions 1–3 and 2–3 leads to the following expressions for transverse-magnetization components under the conditions of two-step resonance (i.e., for $\Omega_1 = \Omega_2 = 0$):

$$M_x = M_{0x} + 2\int_0^\infty dv_z \left(m_1 \cos\frac{\delta z}{v_z} \operatorname{ch}\frac{\varepsilon z}{v_z} + m_2 \sin\frac{\delta z}{v_z} \operatorname{sh}\frac{\varepsilon z}{v_z} + m_3 \operatorname{ch}\frac{\varepsilon z}{v_z} \right), \tag{5.5}$$

$$M_y = M_{0y} - 2\int_0^\infty dv_z \frac{\delta}{\bar{\Delta}} \left(m_1 \sin\frac{\delta z}{v_z} \operatorname{ch}\frac{\varepsilon z}{v_z} - m_2 \cos\frac{\delta z}{v_z} \operatorname{sh}\frac{\varepsilon z}{v_z} \right),$$

where $\delta = (Q^2 + \tilde{\Delta}^2)^{1/2}$.

Here, M_{0i} are components of the spatially-homogeneous magnetization distribution determined by relations (3.2) and (3.4), while the coefficients m_i depend on the nature of the interaction betweeen the active atoms and the cell walls. Thus, in the case of "specularly-noncoherent" reflection from the walls we have

$$m_1 + im_2 = -\frac{\bar{\Delta}}{\delta}(m + im_{0y}) \exp\{-(\varepsilon - i\delta)L/v_z\}, \qquad m_3 = \left(\frac{\bar{\Delta}}{\delta} m - m_{0x}\right) \exp(-\varepsilon L/v_z), \tag{5.6}$$

where

$$m = \frac{\delta\bar{\Delta}(1-\exp(-2\varepsilon L/v_z))\, m_{0x} - Q^2 \sin(2\delta L/v_z) \exp(-2\varepsilon L/v_z)\, m_{0y}}{\delta^2 - (\bar{\Delta}^2 + Q^2\cos(2\delta L/v_z)) \exp(-2\varepsilon L/v_z)},$$

and m_{0i} are the magnetization components in the spatially homogeneous case, given by (3.2).

For "specularly-coherent" reflection of active atoms from the cell walls, the expressions for the coefficients m_i are somewhat simplified:

$$m_1 = \frac{\bar{\Delta}}{\delta} m_{0y} \frac{\sin \delta L/v_z}{\operatorname{sh} \varepsilon L/v_z}, \qquad m_2 = -\frac{\bar{\Delta}}{\delta} m_{0y} \frac{\cos \delta L/v_z}{\operatorname{ch} \varepsilon L/v_z},$$

$$m_3 = 0. \tag{5.7}$$

Figures 9 and 10 illustrate the spatial variation of the transverse magnetization M_y in "specularly-coherent" reflection. The component j_{zy} of the magnetization flux-den-

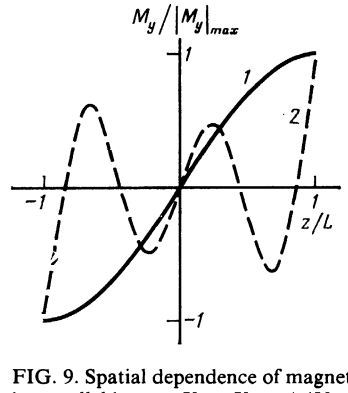

FIG. 9. Spatial dependence of magnetization under two-beam excitation by parallel beams: $U_1 = U_2 = A/50$; 1—$2L = \pi/q$; 2—$2L = 4\pi/q$.

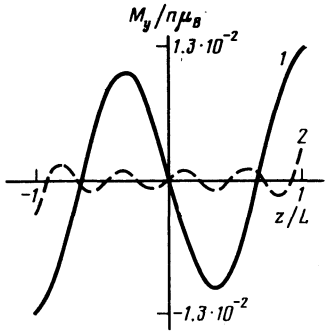

FIG. 10. Spatial oscillations of magnetization under two-beam excitation by parallel beams: $U_1 = U_2 = A/50$; 1—$2L = 3\pi/q$; 2—$2L = 8\pi/q$.

sity tensor is maximum at exact resonance. This is why the corresponding M_y component undergoes a considerable change along the cell axis when $\Omega_1 = \Omega_2 = 0$. At the same time, the transport of other magnetization components reaches a minimum at resonance (or vanishes altogether in the spatially homogeneous case), so that M_x and M_z are constant along the cell.

Let us consider the case of parallel beams. The function $M_y(z)$ is odd. It is monotonic so long as not more than two half-waves of the combined frequency ω_{21} fit within the length of the cell. Increasing the length of the cell breaks up the gas volume into alternating magnetization layers of opposite sign. Thus, we observe the same picture of SQS as in the case of RST. However, the values of transverse magnetization achievable in two-beam excitation are much higher than in RST. Therefore, two-beam excitation provides a higher degree of separation of the mixture of states $|1\rangle$ and $|2\rangle$ into coherent components.

In the case of opposed beams, we have the same oscillatory $M_y(z)$ dependence, but with a very small oscillation period (of the order of $\lambda = 2\pi/k$).

In conclusion, we note that the onset of a macroscopic flux of transverse magnetization under conditions of two-photon resonance and coherent population trapping can be utilized to stabilize the frequency of laser emission by microwave-spectroscopy methods. The physical problems in which the effects investigated in this paper must be taken into account include the problem of the nonlinear intra-Doppler structure of hyperfine transitions of alkaline atoms and the problem of coherent population trapping in a cell of finite optical thickness.

[1]F. Kh. Gel'mukhanov and A. M. Shalagin, Zh. Eksp. Teor. Fiz. **78**, 1674 (1980) [Sov. Phys. JETP **51**, 839 (1980)].
[2]F. Kh. Gel'mukhanov, L. V. Il'ichev, and A. M. Shalagin, Preprint. 1985.
[3]B. D. Agap'ev, M. B. Gornyĭ, and B. G. Matisov, Zh. Eksp. Teor. Fiz. **92**, 1995 (1987) [Zh. Eksp. Teor. Fiz. **65**, 1121 (1987)].
[4]B. D. Agap'ev and B. G. Matisov, Pis'ma Zh. Eksp. Teor. Fiz. **44**, 66 (1986) [JETP Lett. **44**, 81 (1986)].
[5]A. N. Oraevskii, *Molecular Oscillators* [in Russian] Nauka, Moscow, 1964.
[6]K. Blum, *Density Matrix Theory and Its Applications*, Plenum, 1981.
[7]B. D. Agap'ev, *Kinetics of Radio-optical Resonance Line Formation in Alkali Metal Vapors* [in Russian], Leningrad, 1987.
[8]S. Stenholm, *Foundations of Laser Spectroscopy* [Russ. Transl.] Mir, Moscow, 1987.
[9]P. M. Radmore and P. L. Knight, J. Phys. **B, 15**, 561 (1982).

Translated by Simon Kassel